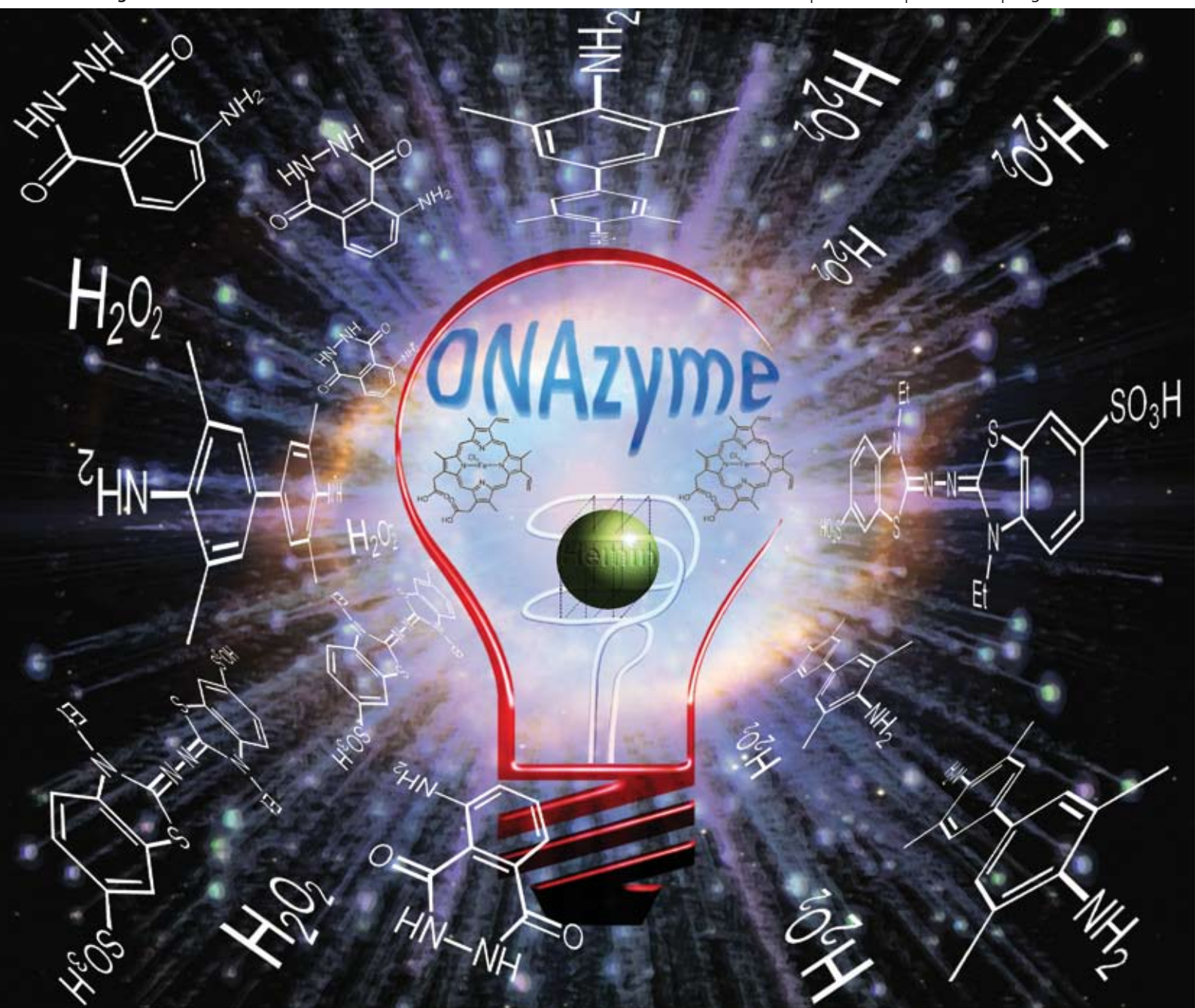


# Chem Soc Rev

Chemical Society Reviews

www.rsc.org/chemsocrev

Volume 37 | Number 6 | June 2008 | Pages 1077–1280



ISSN 0306-0012

RSC Publishing

#### TUTORIAL REVIEW

Itamar Willner, Bella Shlyahovsky, Maya Zayats and Bilha Willner  
DNAzymes for sensing, nanobiotechnology and logic gate applications

#### TUTORIAL REVIEW

C. Oliver Kappe  
Microwave dielectric heating in synthetic organic chemistry

# DNAzymes for sensing, nanobiotechnology and logic gate applications

Itamar Willner, Bella Shlyahovsky, Maya Zayats and Bilha Willner

Received 20th February 2008

First published as an Advance Article on the web 24th April 2008

DOI: 10.1039/b718428j

Catalytic nucleic acids (DNAzymes or ribozymes) are selected by the systematic evolution of ligands by exponential enrichment process (SELEX). The catalytic functions of DNAzymes or ribozymes allow their use as amplifying labels for the development of optical or electronic sensors. The use of catalytic nucleic acids for amplified biosensing was accomplished by designing aptamer–DNAzyme conjugates that combine recognition units and amplifying readout units as in integrated biosensing materials. Alternatively, “DNA machines” that activate enzyme cascades and yield DNAzymes were tailored, and the systems led to the ultrasensitive detection of DNA. DNAzymes are also used as active components for constructing nanostructures such as aggregated nanoparticles and for the activation of logic gate operations that perform computing.

## Introduction

The development of nucleic acids exhibiting selective and specific binding properties towards molecular or protein substrates (aptamers) or the isolation of catalytic nucleic acids (DNAzymes or ribozymes) by the systematic evolution of ligands by exponential enrichment (SELEX) process added important functional nucleic acids for chemical biology, medicine, analytical chemistry and materials science.<sup>1,2</sup> Also, the modification of aptamers or of DNAzymes with chemical functionalities, other than nucleic acids, or alternatively, the conjugation of aptamers and DNAzymes by chemical or biocatalyzed processes yield new functional biomolecular structures that may be employed in various scientific disciplines. Specifically, the modified aptamer and DNAzyme systems can be deposited on surfaces, such as electronic transducers<sup>3</sup> or nanoparticles,<sup>4</sup> and these could then act as stable recognition and catalytic units for the amplified detec-

tion of various analytes. DNAzymes reveal several advantages as compared to enzymes that are commonly used as catalytic labels for amplified biosensing. In contrast to enzymes that are thermally unstable, DNAzymes are impressively stable under ambient and even elevated temperatures. Furthermore, the use of enzymes as catalytic labels requires their chemical conjugation to secondary sensing biomolecules, such as antibodies, avidin or lectins. The association of DNAzyme labels to the sensing sites might be, however, easily accomplished by virtue of the base pairing of nucleobases, and tethering a nucleic acid sequence to the DNAzyme can direct the label to the analyte by hybridization and duplex formation. Finally, in contrast to enzyme labels that require tedious preparation and purification steps, large quantities of DNAzymes may be prepared by the polymerase chain reaction (PCR). Several recent review articles addressed different applications of DNAzymes for sensing and nanotechnology applications.<sup>4,5</sup> The present review article addresses recent developments in the application of DNAzymes as catalysts that transduce and amplify sensing events. We further address the use of DNAzymes as components that read-out the activities of “DNAzyme-machines” or

*Institute of Chemistry, The Hebrew University of Jerusalem, 91904 Jerusalem, Israel. E-mail: willnea@vms.huji.ac.il; Fax: 972-2-6527715; Tel: 972-2-6585272*

*Prof. Itamar Willner, based at The Hebrew University of Jerusalem, has co-authored over 500 research papers and acts as a member of several editorial boards. His research interests include molecular electronics and optoelectronics, nanotechnology, bioelectronics and biosensors, optobioelectronics, nanobiotechnology, supramolecular chemistry, nanoscale chemistry, and monolayer and thin-film assemblies, light-induced electron-transfer processes and artificial photosynthesis.*

*Bella Shlyahovsky completed her BSc and MSc studies in chemistry at the Hebrew University of Jerusalem and joined the*

*laboratory of Prof. I. Willner as a PhD student in 2004. Her research interests include the development of DNA sensors, aptasensors and immunosensors. She is also involved in the application of aptamers and DNAzymes as components for the design of logic gates and biocomputing systems. She is the recipient of the Ministry of Science Fellowship for graduate students.*

*Dr. Maya Zayats studied chemistry at the Hebrew University of Jerusalem. After completing her BSc she joined the laboratory of Prof. I. Willner to carry out her PhD studies. She is the recipient of the Eshkol Fellowship (Israel Ministry of*

*Science) as well as the Yashinski Award. Her research interests include the development of enzyme-based electronic biosensors and the application of nanoparticles for sensing.*

*Dr Bilha Willner acts as a Senior Research Associate in the laboratory of Prof. I. Willner. She completed her PhD studies at the Hebrew University of Jerusalem in the area of organometallic chemistry. Her scientific interests include bioelectrochemistry, biosensors, assembly of nanoparticles on surfaces and nanobiotechnology.*

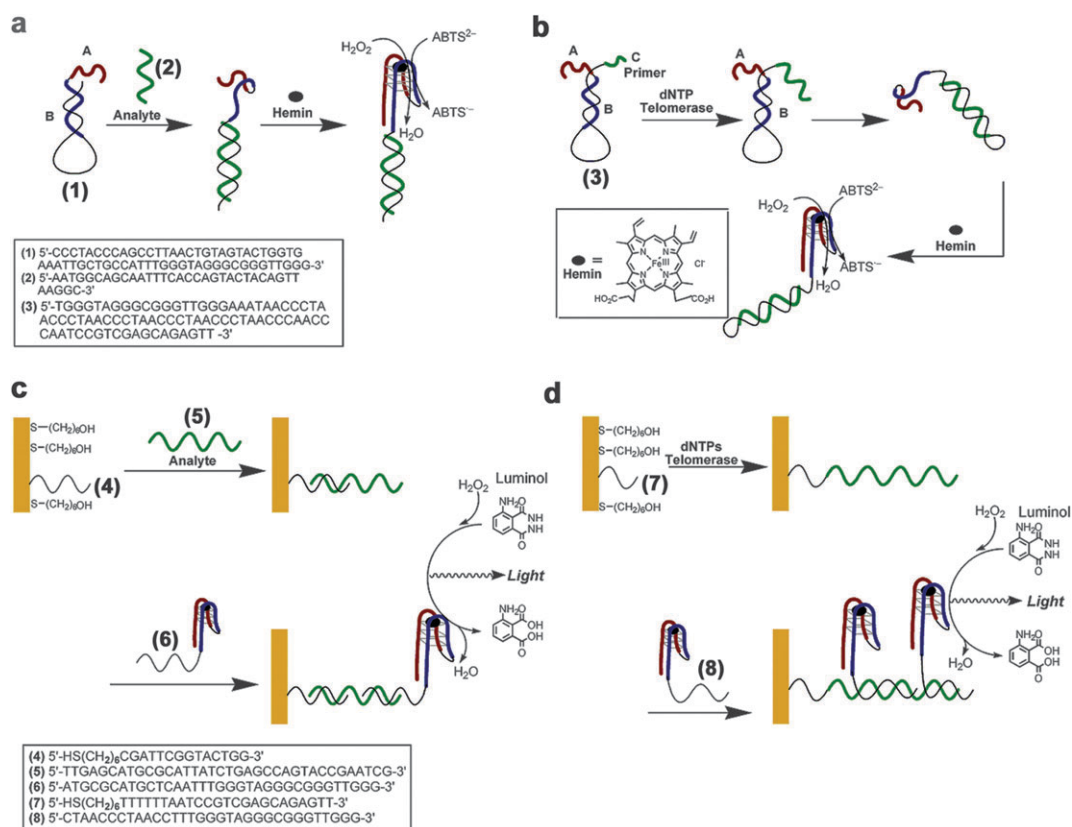


**Fig. 1** (a) Analysis of a DNA by a hairpin that generates the horseradish peroxidase-mimicking DNAzyme. (b) Detection of telomerase activity by a hairpin structure that yields the horseradish peroxidase-mimicking DNAzyme. (Reprinted with permission from ref. 10. Copyright 2004, American Chemical Society). (c) and (d) The chemiluminescence analysis of DNA or telomerase activity on surfaces by the use of nucleic acid-functionalized DNAzyme units as labels. (Reprinted with permission from ref. 13. Copyright 2004, American Chemical Society).

as units that perform logic gate operations. Lastly, we will also discuss the utility of DNAzymes in nanobiotechnology.

### Amplified sensing with DNAzymes: DNA and telomerase detection

An interesting DNAzyme that is frequently used for biosensing is a biocatalytic nucleic acid with peroxidase mimicking catalytic activity.<sup>6,7</sup> In this molecule, the complexation of hemin with a guanine-rich single-stranded nucleic acid yields a G-quadruplex structure that catalyzes the oxidation of 2,2'-azino-bis(3-ethylbenzothiazoline)-6-sulfonic acid (ABTS<sup>2-</sup>) by H<sub>2</sub>O<sub>2</sub> to form the respective colored radical product, ABTS<sup>•-</sup>.<sup>8</sup> It was also demonstrated that the hemin/G-quadruplex structure catalyzes the oxidation of luminol by H<sub>2</sub>O<sub>2</sub> and the generation of chemiluminescence.<sup>9</sup> This DNAzyme was used for the colorimetric or chemiluminescent detection of nucleic acids, or to follow the activity of telomerase, a versatile marker for cancer cells.<sup>10</sup> Fig. 1 outlines several configurations that were employed for the analysis of nucleic acids. By one approach<sup>10</sup> (Fig. 1(a)), a hairpin structure (1) was designed to include in its single-stranded loop the recognition sequence for analyzing the target DNA (2), and in its hybridized stem a nucleic acid sequence consisting of a single-stranded part, A, tethered to a second sequence, B, that is hybridized in the stem configuration. While the domains A and B provide the

sequences for the assembly of the hemin/quadruplex DNAzyme structure, the formation of the catalytic DNA is thermodynamically prohibited due to the stability of the stem duplex. The hybridization of the analyte (2) with the loop region opened, however, the stem duplex, resulting in the formation of the hemin/G-quadruplex structure that catalyzed the oxidation of ABTS<sup>2-</sup> to the colored oxidized ABTS<sup>•-</sup> product ( $\lambda = 414 \text{ nm}$ ,  $\epsilon = 3.6 \times 10^4 \text{ M}^{-1} \text{ cm}^{-1}$ ). A similar approach was used to follow telomerase activity<sup>10</sup> (Fig. 1(b)). Telomeres are G-rich nucleic acids consisting of constant repeat units that are positioned at the ends of the chromosomes. They protect the chromosomes, and participate in signaling cell proliferation, and the termination of cell life cycle.<sup>11</sup> Telomerase, is a ribonucleoprotein that appears in certain cells and it catalyzes the synthesis of the telomeres. This transforms the cells into immortal units, and hence, is considered as a versatile marker for cancer cells.<sup>12</sup> A hairpin structure (3) included in its single-stranded loop the complementary sequence to the telomere units. The "stem" included in one strand the domains A and B that self-assemble to the G-quadruplex horseradish peroxidase-mimicking DNAzyme, where to the other end of the stem was tethered the nucleic acid sequence C, that is recognized by telomerase. The duplex structure of the stem prohibits the self-assembly of the DNAzyme due to its stability. In the presence of telomerase and the nucleotide mixture dNTPs, the tether C was elongated to yield the telomeres. The latter

generated sequence hybridized with the loop region. This led, in the presence of hemin, to the self-assembly of units A and B to the DNAzyme that led to the biocatalyzed oxidation of ABTS<sup>2-</sup> by H<sub>2</sub>O<sub>2</sub> and to the colorimetric detection of the activity of telomerase.

The biocatalyzed generation of chemiluminescence by the hemin/G-quadruplex DNAzyme was further used to develop surface-confined assays for the detection of DNA or telomerase activity.<sup>13</sup> The DNAzyme was tethered to a nucleic acid sequence (6) that is complementary to a single-stranded domain of the analyte nucleic acid (5), hybridized to the primer DNA (4) on the surface. The nucleic acid tethered to the DNAzyme (6) acted as a label for the chemiluminescent detection of the hybrid between the DNA analyte (5) and the capturing nucleic acid (4) that were confined to a gold-coated glass support (Fig. 1(c)). The DNA could be analyzed with a detection limit that corresponded to  $1 \times 10^{-9}$  M. Similarly, a label that consisted of the DNAzyme and a nucleic acid tether complementary to the telomere units was used for the detection telomerase activity (Fig. 1(d)). The primer (7) associated with the gold surface was elongated by the interaction with telomerase, which was extracted from HeLa cancer cells, in the presence of the dNTPs mixture. The hybridization of the DNAzyme label units (8) with the chains generated by telomerase enabled the chemiluminescent detection of telomerase activity extracted from only 1000 HeLa cells. The sensitivities of the latter DNA and telomerase activity sensors were improved by the use of gold nanoparticles as carriers for the DNAzyme labels.<sup>14</sup> The hybridization of the DNAzyme-functionalized gold nanoparticles with the analyte DNA or the telomerase-generated telomere chains resulted in multi-labels of the DNAzyme units for a single DNA recognition event, or single telomerization process, thus, establishing doubly-amplified colorimetric or chemiluminescence surface-confined sensors.

DNAzymes exhibiting nucleic acid cleavage activities in the presence of added cofactors have been elicited and used for the specific scission of DNA sequences. For example, nucleic acid sequences that specifically bind Pb<sup>2+</sup>, Mg<sup>2+</sup> or Cu<sup>2+</sup> ions, UO<sub>2</sub><sup>+</sup>,<sup>15-18</sup> or histidine<sup>19</sup> were found to yield supramolecular coiled structures that cleave specific DNA sequences. Using these properties, pre-designed nucleic acid sequences were tethered to the DNAzyme structures to yield functional units for the amplified detection of the cofactors, or alternatively, for target DNA/RNA units. The optical amplified detection of a target DNA (9) by the nucleic acid-cleaving DNAzyme is depicted in Fig. 2.<sup>20</sup> The probing DNAzyme (10) consisted of three regions: a recognition domain (red), a DNAzyme folding region (blue) and a sequence-specific cleavage site (green). The cleavage site was functionalized at its two ends with a pair of donor-acceptor FRET dyes. Hybridization of the target DNA (9) with the probe nucleic acid (10) stabilized the duplex structure, and the folded DNAzyme domain, that in the presence of Mg<sup>2+</sup>, cleaved the specific base site. This separated the fluorescent-dye reporting nucleic acid, and resulted in the separation of the original (9)/(10) structure due to the elimination of allosteric duplex stabilization. The release of the target recycled the cleavage ability of the probe nucleic acid, and the released fluorophore-functionalized nucleic acid sequence

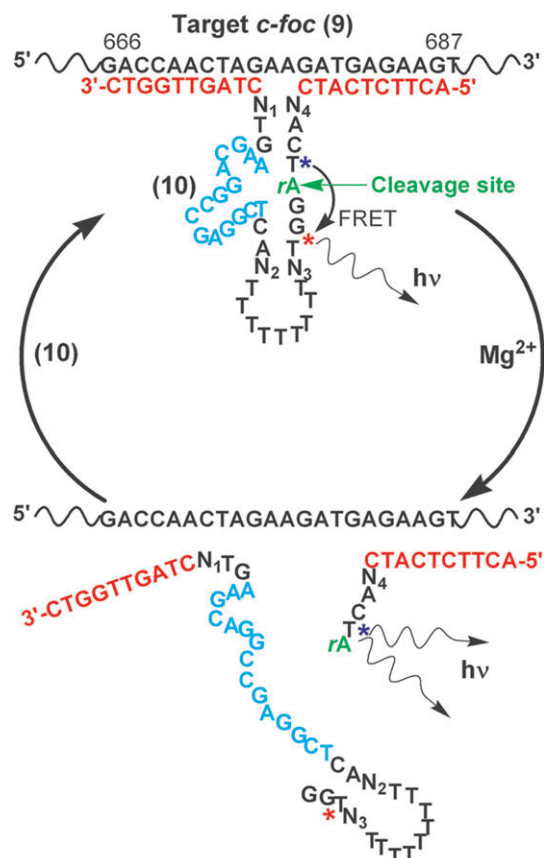


**Fig. 2** Analysis of a target DNA by the use of Mg<sup>2+</sup>-dependent DNAzyme that undergoes self-cleavage and yields a fluorescent product. (Reprinted in part with permission from ref. 20. Copyright 2003, American Chemical Society).

acted as reporter for the analyzed DNA (9). This method was successfully applied to analyze the c-fos 666-687 sequence.

The Pb<sup>2+</sup>-activated DNAzyme was often used for the amplified detection of Pb<sup>2+</sup> ions (Fig. 3). Lead ions are common pollutants in paints, ceramics, and water resources. Low concentrations of Pb<sup>2+</sup> act as severe poisons that damage the neural response system and organs such as the liver, and thus, its rapid and sensitive detection is significant. One approach,<sup>21</sup> included the use of the Pb<sup>2+</sup>-dependent RNA-cleaving DNAzyme 17E (11) as a biocatalyst that stimulated the de-aggregation of Au nanoparticles through a cleavage process thus providing a colorimetric sensor for Pb<sup>2+</sup> (Fig. 3(a)). The nucleic acid (12) included the RNA cleavage site and the base sequences that hybridize with the Pb<sup>2+</sup>-dependent DNAzyme 17E (11). To the 3' and 5' ends of the cleavable nucleic acid were tethered nucleic acid sequences complementary to the nucleic acid (13) functionalizing Au nanoparticles. The Au nanoparticles were then aggregated by the bridging cleavable nucleic acid (12), while the DNAzyme was hybridized with the single-stranded domain of (12). Bridging of the Au nanoparticles by the nucleic acid (12) resulted in the formation of an Au nanoparticles aggregate, reflected by the blue color ( $\lambda = 700$  nm) of the system as a result of an interparticle coupled plasmon. Addition of Pb<sup>2+</sup> activated the DNA-cleaving DNAzyme, and the scission of (12) at the RNA

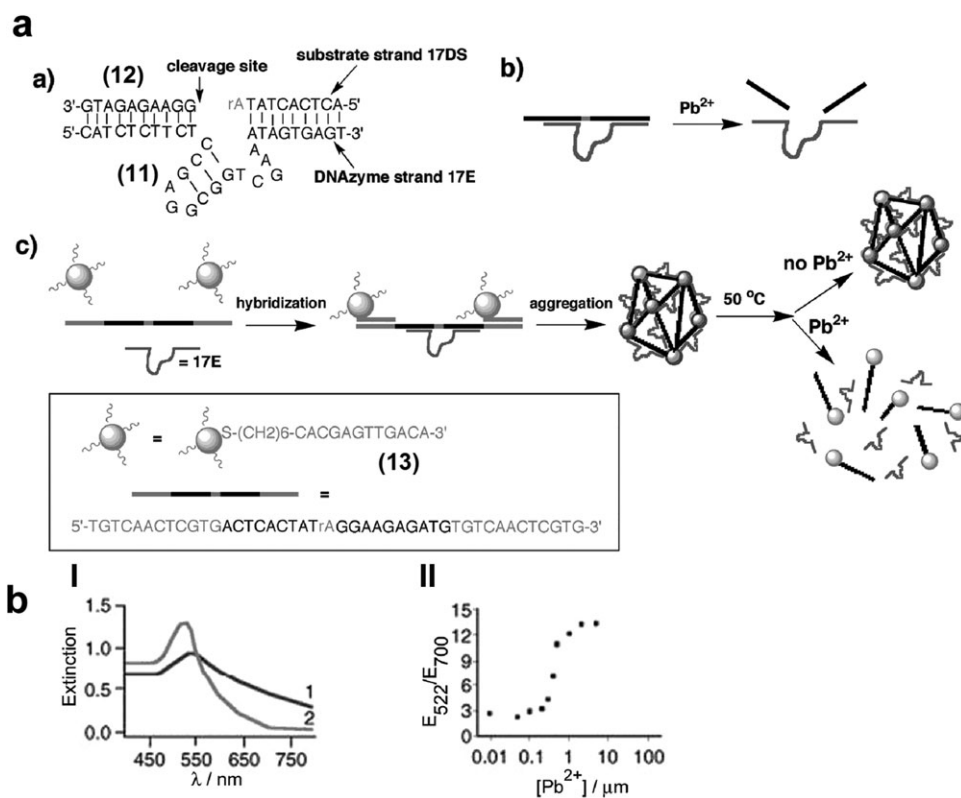


**Fig. 3** (a) Analysis of  $\text{Pb}^{2+}$  by the de-aggregation of an Au nanoparticles aggregate by means of the  $\text{Pb}^{2+}$ -dependent DNAzyme. (b) (I) Absorbance spectra of: (1) The Au nanoparticle aggregate and (2) the Au separated nanoparticles generated by the  $\text{Pb}^{2+}$ -dependent DNAzyme. The spectra were recorded in the absence, curve 1, or in the presence, curve 2, of  $\text{Pb}^{2+}$  ions ( $5 \mu\text{M}$ ). (II) Calibration curve corresponding to the absorbance ratio of separated Au nanoparticles/aggregated Au nanoparticles at different concentrations of  $\text{Pb}^{2+}$  (Reprinted with permission from ref. 21. Copyright 2003, American Chemical Society).

nucleobase. This resulted in the separation of the cleaved units from the Au nanoparticles, a process that led to the de-aggregation of the particles that exhibited the red color ( $\lambda = 522 \text{ nm}$ ) characteristic to the individual Au nanoparticles (Fig. 3(b)). The extent of de-aggregation of the gold nanoparticles and thus the color changes of the system, were controlled by the concentration of  $\text{Pb}^{2+}$ . The system enabled the detection of  $\text{Pb}^{2+}$  with a sensitivity that corresponded to  $5 \times 10^{-7} \text{ M}$ .

The  $\text{Pb}^{2+}$ -dependent DNAzyme was also immobilized on surfaces, and optical<sup>22</sup> or electrochemical<sup>23</sup> assays for detecting  $\text{Pb}^{2+}$  by the DNAzyme were developed. This will enable in the future the development of DNAzyme-based electrical sensing devices and the fabrication of DNAzyme-based optical sensing chips. The thiolated 17E  $\text{Pb}^{2+}$ -dependent DNAzyme functionalized with the dabcyll dye (14) was assembled on Au surfaces,<sup>22</sup> and the surface was blocked with mercaptohexanol to prevent non-specific interactions with the gold support. The resulting modified surface was hybridized with the RNA nucleobase-containing substrate that was modified at its end with fluorescein (15) (Fig. 4(a)). In the hybrid configuration the fluorescence of fluorescein was quenched. The cleavage of the substrate in the presence of  $\text{Pb}^{2+}$  released a short fluorescence tethered nucleic acid, and the fluorescence of the solution provided a quantitative signal for the DNAzyme activity and the concentration of  $\text{Pb}^{2+}$ . This method revealed a linear

calibration curve for the analysis of  $\text{Pb}^{2+}$  in the region of  $10 \mu\text{M} \geq [\text{Pb}^{2+}] \geq 1 \text{ nM}$ .

A related electrochemical system for the detection of  $\text{Pb}^{2+}$  was demonstrated<sup>23</sup> (Fig. 4(b)). The 5'-thiolated  $\text{Pb}^{2+}$ -dependent DNAzyme modified at its 3'-end with the redox-active unit methylene blue (MB), (16), was immobilized on Au electrodes, and the RNA nucleic acid nucleobase-containing substrate (17) was hybridized with the DNAzyme. The “stiff” duplex structure of the DNAzyme–substrate prohibited electrical contact between the redox label and the electrode. In the presence of  $\text{Pb}^{2+}$ , the cleavage of the substrate occurred, and the duplex was separated. The flexibility of the MB-modified single-stranded DNA facilitated the electrochemical communication between the redox label and the electrode, and the resulting voltammetric response provided a signal for the quantitative analysis of  $\text{Pb}^{2+}$ . This method enabled the analysis of  $\text{Pb}^{2+}$  with a detection limit that corresponded to  $3 \times 10^{-7} \text{ M}$  (62 ppb) with an impressive selectivity. The  $\text{Pb}^{2+}$ -dependent DNAzyme was also applied to analyze  $\text{Pb}^{2+}$ -ions using a microfluidic chip module.<sup>24</sup> The DNAzyme strand, attached to the chip, was modified at its 3'-end with a Dabcyll quencher, and blocked by the substrate functionalized at its 3' and 5' ends with Dabcyll and the FAM-fluorophore, respectively. Within this structure, the fluorescence of FAM was quenched, but the addition of  $\text{Pb}^{2+}$  cleaved the substrate, and

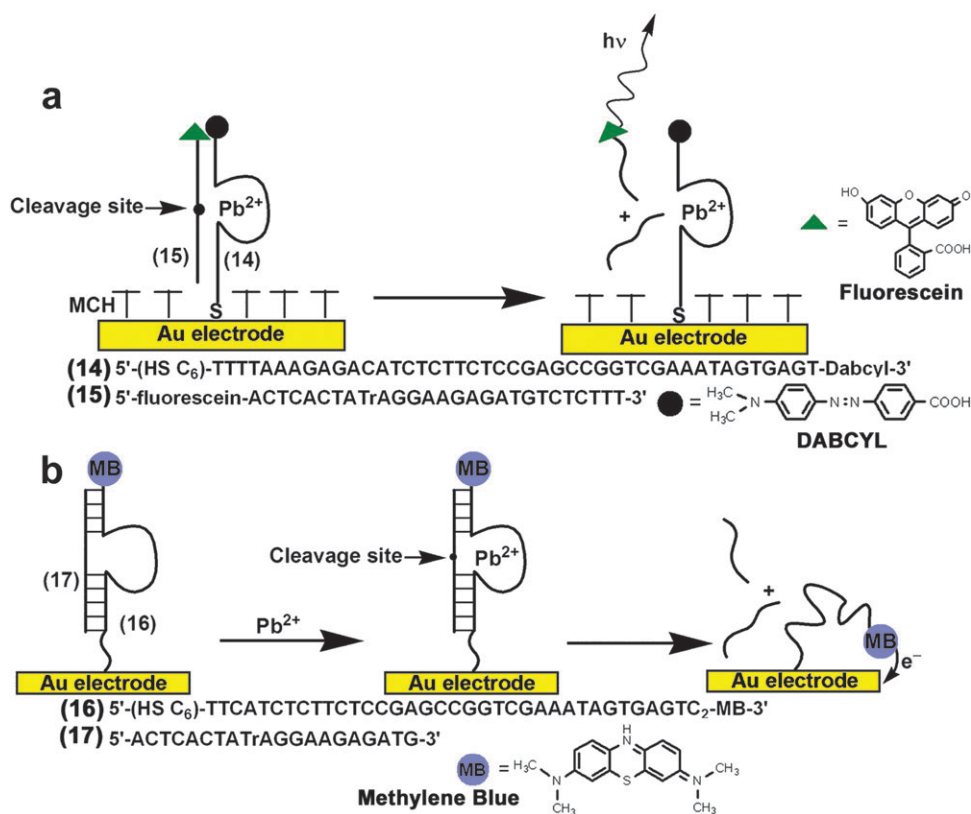


**Fig. 4** (a) Optical detection of  $Pb^{2+}$  by the cleavage of a fluorophore-functionalized substrate by the  $Pb^{2+}$ -dependent DNAzyme that releases a fluorophore-functionalized nucleic acid product. (b) Electrochemical detection of  $Pb^{2+}$  by the cleavage of a duplex DNA structure by the  $Pb^{2+}$ -dependent DNAzyme and the formation of a redox-tethered single-stranded nucleic acid that electrically communicates with the electrode. (Adapted with permission from ref. 23. Copyright 2007, American Chemical Society).

triggered on the fluorescence of the fluorophore. Other metal-dependent DNAzymes are available, and for example, a  $Cu^{2+}$ -specific DNAzyme was similarly used to analyze  $Cu^{2+}$  ions.<sup>25</sup>

### Aptamer–DNAzyme conjugates for biosensing

Nucleic acids sequences that recognize different classes of analytes were isolated by the SELEX process, and these are known as aptamers. For example, aptamer recognizing low-molecular-weight substances such as cocaine,<sup>26</sup> bioactive cofactors such as  $NAD^+$ ,<sup>27</sup> the flavin cofactor<sup>28</sup> or adenosine triphosphate (ATP)<sup>29</sup> were prepared. Also, aptamers against various proteins such as the HIV reverse transcriptase<sup>30</sup> or toxins such as staphylococcal enterotoxin B<sup>31</sup> were produced. The availability of the different aptamers suggests that their binding to DNAzyme units might lead to bifunctional nucleic acid conjugates that include in the same molecular structure a recognition site and a catalytic reporting unit that provides the readout signal.

An aptamer–DNAzyme hybrid system that included the  $Pb^{2+}$ -dependent catalytic nucleic acid was applied to analyze adenosine monophosphate<sup>32</sup> by applying the DNAzyme-mediated de-aggregation of Au NPs as optical readout signal (Fig. 5(a)). The  $Pb^{2+}$ -dependent DNAzyme sequence (18) was partially complementary to the nucleic acid (19) that included the anti-adenosine aptamer region. Hybridization of the DNAzyme with the aptamer-containing nucleic acid (19)

blocked the formation of the DNAzyme catalytic configuration. The 5' and 3' ends of the DNAzyme and the aptamer, respectively, were complementary to the substrate (20) that included the RNA nucleobase that is cleavable by the DNAzyme and its two ends that were complementary to the (21)- and (22)-functionalized Au nanoparticles, respectively. Under these collective complementarities of the components, the Au nanoparticles underwent aggregation that yielded a blue color originating from the coupled interparticle plasmon. In the presence of adenosine monophosphate, and  $Pb^{2+}$ -ions as cofactor, the de-aggregation of the Au nanoparticles was controlled by the concentration of adenosine, and as its concentration increased, the extent of aggregation diminished, a process that was followed by the increase in the red absorbance features of individual Au nanoparticles. In this latter system, adenosine stimulated the separation of the blocked DNAzyme/aptamer (18)/(19) structure while forming the aptamer–substrate complex. This activated the  $Pb^{2+}$ -dependent scission-DNAzyme that cleaved (20) at the RNA nucleobase. As a result, all collective hybridization features were lost, and the thermal melting of the individual hybrid units led to the de-aggregation of the nanoparticles. The color changes in the system originating upon de-aggregation of the gold nanoparticles enabled the analysis of adenosine monophosphate with a sensitivity that corresponded to  $1.2 \times 10^{-6}$  M.

A related conjugate of the anti-adenosine aptamer-HRP-mimicking DNAzyme (23) was used for the colorimetric or

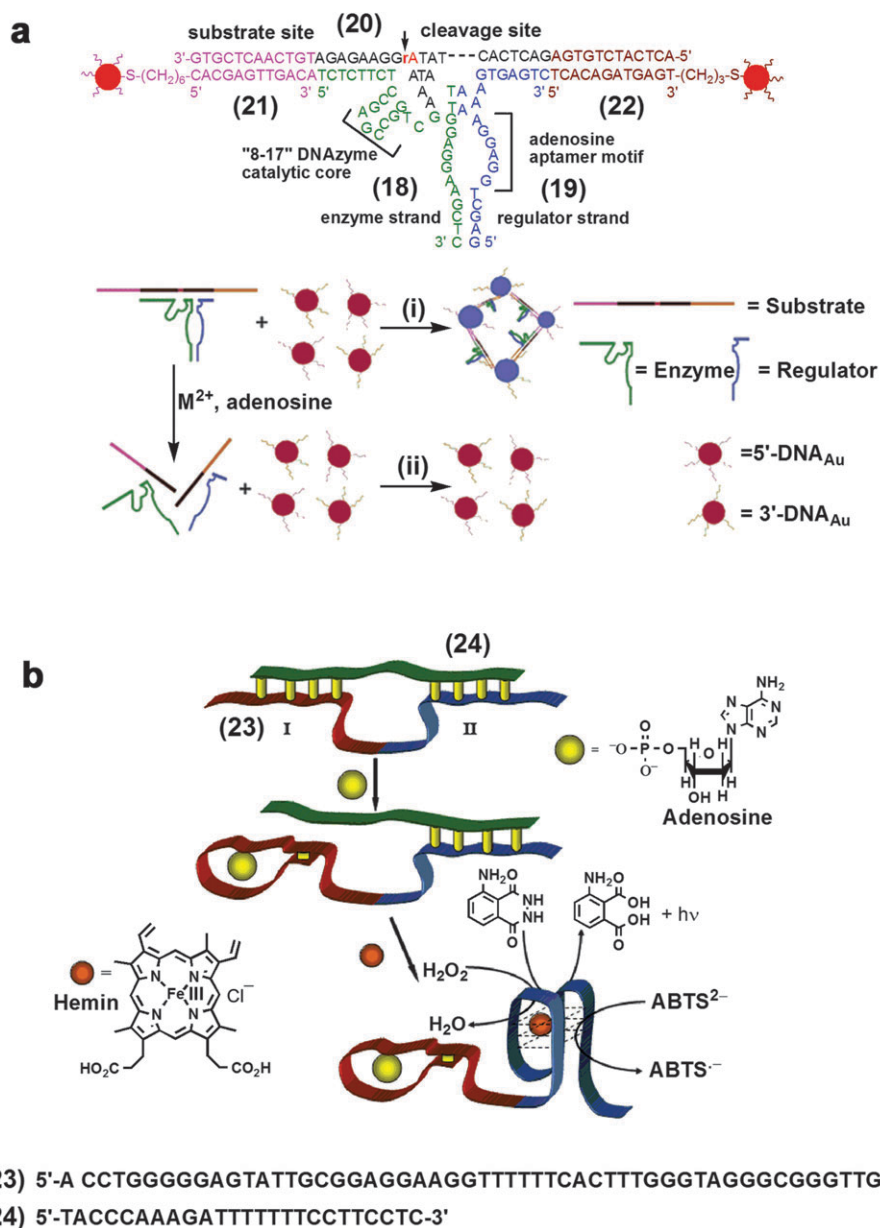


**Fig. 5** (a) Aggregation of Au NPs by a supramolecular bridging complex consisting of the Pb<sup>2+</sup>-dependent DNAzyme and the adenosine aptamer that are blocked by the substrate (20). The separation of the Au NPs is stimulated by the addition of Pb<sup>2+</sup> and adenosine that results in the separation of the aptamer–adenosine complex and the cleavage of the substrate. Adenosine mono phosphate is detected colorimetrically by following the absorbance changes upon the transition of the Au NP aggregate to separated Au NPs. (Reprinted with permission from ref. 32. Copyright 2004, American Chemical Society). (b) The optical detection of adenosine by an aptamer–DNAzyme conjugate that is blocked by a nucleic acid into a catalytic inactive structure. The formation of the aptamer–adenosine complex releases the horseradish peroxidase-mimicking DNAzyme that permits the optical readout of the formation of the aptamer–adenosine complex. (Reprinted with permission from ref. 33. Copyright 2007, American Chemical Society).

chemiluminescent detection of adenosine (Fig. 5(b)).<sup>33</sup> The active DNAzyme structure was blocked by the hybridization of the 3' and 5' ends of the aptamer and DNAzyme units with the nucleic acid (24) that is partially complementary to the DNAzyme sequence, and partially complementary to the aptamer regions. Dehybridization of the aptamer in the presence of added adenosine through the formation of the aptamer–adenosine complex induced the separation of the

DNAzyme sequence that self-assembled, in the presence of hemin, to the active horseradish peroxidase-mimicking DNAzyme. This provided the colorimetric or chemiluminescence readout signals for the formation of the aptamer–analyte complex by the H<sub>2</sub>O<sub>2</sub>-mediated oxidation of ABTS<sup>2-</sup>, or by the biocatalyzed generation of light in the presence of H<sub>2</sub>O<sub>2</sub>/luminol, respectively. This method paves the way to construct a catalytic DNAzyme–aptamer sensing conjugate for any low-

molecular-weight or macromolecular analyte for which an aptamer exists.

### Amplified sensing by enzyme-stimulated synthesis of DNAzymes

Nucleic acids include in their nucleobase sequences substantial encoded information that is reflected in the stability of the duplex formation with complementary oligonucleotide sequences, in the self-organization of the nucleic acids into complex two- or three-dimensional structures,<sup>34,35</sup> in the specific binding of intercalators or metal ions, and in the self-assembly into binding (aptamers) or catalytic (DNAzyme) structures. Furthermore, the nucleobase order controls biocatalytic processes on the DNA, and the cleavage or nicking of duplex DNAs at sequence-specific domains represent topological reactivities of oligonucleotide structures. All of these properties were recently used to develop “DNA-based machines” that perform mechanical functions such as “walking”, “scission” or “rotation” as a result of an external triggering signal.<sup>36–38</sup> The concept of “DNA machines” may be further adapted to develop highly sensitive DNA detection schemes that could provide isothermal analytical methods for the substitution of the PCR (Polymerase chain reaction) process. The autonomous enzyme-stimulated mechanical synthesis of DNAzyme units that is triggered by a recognition event of the analyte substrate on a nucleic acid “track” represents a two-phase amplification process for the sensing reaction. In the first step, the recognition of the analyte triggers the biocatalytic formation of numerous DNAzyme units on the nucleic acid “track”. In the second amplification step, the synthesized DNAzyme units exhibit biocatalytic reporter properties, and numerous readout signals are generated. Thus, a single recognition event is translated through the two amplification steps into numerous transduction signals.

The hybridization of an analyte DNA with a sequence-designed circular DNA was used to activate the rolling circle amplification (RCA) process that resulted in the synthesis of DNAzyme units of peroxidase activity,<sup>39</sup> and the method was applied to analyze the M13 phage DNA.<sup>40</sup> A circular DNA, (25), that included a nucleic acid sequence for capturing the analyte, domain A, and three nucleic acid domains B, C, and D complementary to the horseradish peroxidase-mimicking DNAzyme, was constructed (Fig. 6(a)). A nucleic acid hairpin structure (26) that included in its single-stranded loop domain a recognition sequence was used to capture the M13 phage DNA analyte (27). Upon hybridization of the analyte with the loop domain, the hairpin opened. The released single-stranded stem residue was designed to hybridize with the recognition sequence of the circular DNA. In the presence of polymerase and the dNTPs mixture, the replication and the rolling circle amplification were initiated. In each revolution three DNAzyme units that bind hemin were generated. AFM measurements indicated that DNAzyme chains as long as 10  $\mu\text{m}$  were formed. Fig. 6(b) and (c) show the color changes and the resulting light intensities observed upon analyzing different concentrations of M13 phage DNA. The detection limit for analyzing the target DNA corresponded to  $1 \times 10^{-14}$  M.<sup>40</sup> This sensing approach is generic and might be applied to

analyze any target DNA while applying the same circular DNA, (25) and a hairpin with a variable single-stranded loop, yet with an identical stem structure to (26).

A different DNA machine for the amplified analysis of DNA is depicted in Fig. 6(d), and it involves the autonomous synthesis of the peroxidase-mimicking DNAzyme.<sup>41</sup> This is exemplified with the analysis of the M13 phage DNA (27). A nucleic acid “track” (28), was constructed, and it included three active domains: the region I acted as the recognition site, whereas region III was complementary to the horseradish peroxidase-mimicking DNAzyme sequence. The region II was encoded with the sequence that controls upon recognition the replication of the “track” and the formation of the nicking sites for the evolution of the DNAzyme units. The hairpin structure (29) was used to capture in its single-stranded loop the analyte M13 phage DNA (27). The hybridization of the analyte with the hairpin opened the stem region, and the generated 3'-end of the stem complemented the recognition domain I of the “track” (28). The hybridization of the (27)/(29) hybrid to the recognition sequence activated in the presence of polymerase and the dNTPs mixture the replication of the “track”. The latter biocatalytic reaction resulted in the formation of the nucleobase sequence for nicking by the N. BbvC 1A enzyme that cleaved the replicated strand. This, however, initiated the autonomous synthesis of the DNAzyme by the polymerase-induced replication of the track and concomitant displacement of the cleaved strand (30) that self-assembled, in the presence of hemin, to the horseradish peroxidase-mimicking DNAzyme. Fig. 6(e) and (f) depict the colorimetric changes and light intensities generated by the evolved DNAzymes upon analyzing different concentrations of the M13 phage DNA. The analyte was detected with sensitivity that corresponded to  $1 \times 10^{-14}$  M (with a signal-to-noise ratio of *ca.* 3).

A method that adapted concepts of the real-time polymerase chain reaction (RT-PCR) that uses the horseradish peroxidase-mimicking DNAzyme as a generator of an optical readout signal, was developed.<sup>42</sup> The real-time PCR method is the most efficient procedure for the quantified, *in situ*, analysis of DNA, and it includes the fluorescent transduction of the progress of the replication process.<sup>43</sup> The conjugation of a DNAzyme probes as catalytic transducing units of PCR processes might not only provide a method to substitute the expensive RT-PCR fluorescent labels, but add an additional amplification step to the PCR reaction, thus enhancing the sensitivity and shortening the analysis time-intervals. Fig. 7 exemplifies the DNAzyme-stimulated PCR analysis of the M13 phage DNA target.<sup>42</sup> A primer, (31), was designed, consisting of a capture nucleic acid that was conjugated to a sequence complementary to the horseradish peroxidase-mimicking DNAzyme. This acted as a blocker unit for the tethered DNAzyme sequence, where the blocker and the DNAzyme were separated by an oligoethylene glycol bridge. Under these conditions, the DNAzyme sequence was inaccessible, and its folding into the biocatalytically active structure was prohibited. In the presence of polymerase and dNTPs, replication was induced, and the thermally separated product (32), was hybridized with the primer (33) that included a similarly blocked DNAzyme sequence. By the reverse







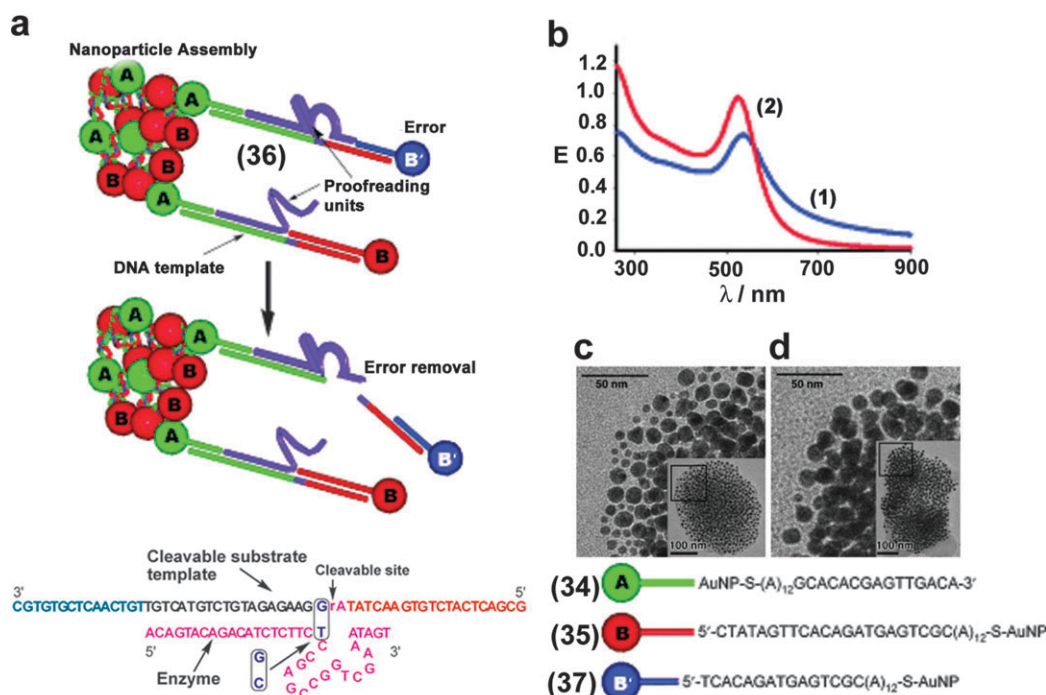


**Fig. 8** (a) Error-correction and removal within aggregated Au NPs using the  $\text{Pb}^{2+}$ -dependent DNAzyme. (b) Absorbance spectra of: (1) Error-containing Au NP aggregates. (2) Au NP aggregate after error removal. (c) and (d) TEM images of the Au NP aggregates before and after error removal, respectively. (Reproduced with permission from ref. 45. J. Liu *et al.*, Proofreading and error removal in a nanomaterial assembly, *Angew. Chem., Int. Ed.*, 2005, **44**, 7290. Copyright 2005, Wiley-VCH Verlag GmbH & Co. KGaA).

type B' from the aggregate. The error removal was confirmed by absorbance spectroscopy (Fig. 8(b)) and TEM images (Fig. 8(c) and (d)).

Structured nucleic acids have been recently used for logic gate and computational operations. Logic gates provide the functional units of computers. For binary computing logic gates are activated by two electrical inputs that regulate the electrical output, and the combination of several gates permits computations. Recent research efforts use molecules<sup>46</sup> or biomolecules<sup>47</sup> as functional components that are triggered by external stimuli such as light, pH, electrical or chemical inputs to perform logic operations. Different applications of molecular or biomolecular computing systems were suggested, and, for example, enzyme-based logic gate systems were reported as potential computers to follow metabolic pathways.<sup>47</sup> Similarly, DNA-based computers attracted recent research efforts, and the clinical impact of these systems was discussed.<sup>48</sup> Biocatalytic transformations of DNA templates, or binding of low-molecular-weight substrates to aptamers were used as computational elements<sup>49,50</sup> or as systems that perform logic gate operations.<sup>51,52</sup>

DNAzyme structures were used to construct different logic gates, and to perform arithmetic operations. For example, the nucleic acid construct (38) was designed to include the E8-17 deoxyribozyme construct (green) that was constrained into an inactive catalytic structure due to the formation of two hairpin structures (Fig. 9(a)).<sup>53</sup> The treatment of the structure (38) with the nucleic acid (39) that acted as one input,  $i_1$ , resulted in the opening of the "left" hairpin by hybridization to the input, but the deoxyribozyme remained inactive. Similarly, treatment of (38) with the nucleic acid (40) that acted as second input,  $i_2$ ,

resulted in the opening of the "right" hairpin structure, but the resulting deoxyribozyme was not activated. Treatment, however, of the structure (38) with the two inputs,  $i_1$  and  $i_2$ , opened both of the hairpin structures, and this released the active deoxyribozyme structure, in the presence of the nucleic acid (41) that acted as substrate for the ribozyme. The cleavage of the hybridized substrate resulted in short sequence hybridization products that were thermally dissociated from the deoxyribozyme backbone. To the substrate (41) were tethered a fluorophore (fluorescein) and a black-hole quencher (BH<sub>1</sub>). The fluorophore was quenched in the intact substrate structure (41), but the cleavage of the substrate by the deoxyribozyme, and the dissociation of the two cleaved fragments separated the fluorophore and quencher, and this activated the fluorescence of fluorescein,  $\lambda_{\text{ex}} = 480 \text{ nm}$ ;  $\lambda_{\text{em}} = 530 \text{ nm}$ . Thus, the activation of the fluorescence from the system occurred only if the template was subjected to the two input signals,  $i_1$ ,  $i_2$ , resulting in an "AND" logic gate. The construction of the "XOR" logic gate, where two "true" inputs ("1") yield a "false" output ("0"), is depicted in Fig. 9(b). The nucleic acid (42) was used as template that performs the function of this logic gate. The template included two inactive deoxyribozyme units that were blocked to "mute" structures by two hairpin structures A and B that partially hybridized with the deoxyribozyme sequences. The two deoxyribozyme units were further linked to the two hairpin structures C and D that acted as "regulator" units that control the communication between the two catalytic nucleic acids. The addition of the nucleic acid (39) as input  $i_1$  resulted in the hybridization to hairpin A and its opening, and the concomitant hybridization to hairpin D and its opening. While the opening of hairpin A activated the

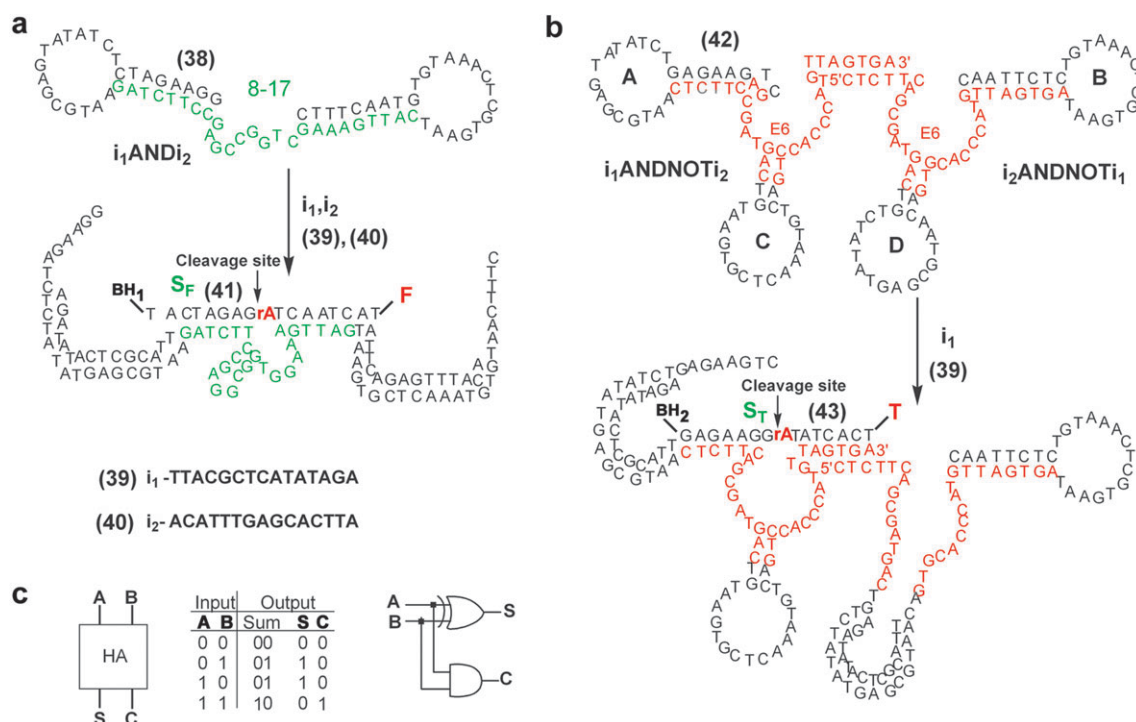


**Fig. 9** Logic gates generated by nucleic acid constructs that include a DNAzyme unit that cleaves the appropriate substrates that yield a fluorescence readout signal of the logic gate operations: (a) The “AND” gate. (b) The “XOR” gate. (c) The truth table and schematic electronic circuit corresponding to the half-adder that originates from the combined “AND” and “XOR” gates. (Reprinted with permission from ref. 53. Copyright 2003 American Chemical Society).

catalytically active structure of the “left” deoxyribozyme, the opening of hairpin D distorted the “right” deoxyribozyme to a catalytically inactive structure. Treatment of the resulting structure with the reporter substrate (43) resulted in its cleavage by the “left” deoxyribozyme, and the separation of the short nucleic acid products. The substrate (43) was modified at its two ends with the fluorophore TAMRA and the black-hole quencher BH<sub>2</sub>, resulting in the intramolecular quenching of the fluorophore. The catalytic scission of the substrate resulted in, however, the separation of the fluorophore quencher units, thus activating the fluorescence from TAMRA,  $\lambda_{\text{ex}} = 530 \text{ nm}$ ;  $\lambda_{\text{em}} = 580 \text{ nm}$ , that provided the readout signal for the logic gate operation. Thus, the treatment of the template (42) with the inputs (1, 0) resulted in the true output “1”. Similarly, the treatment of the template (42) with the nucleic acid (40) acting as input  $i_2$  resulted in the hybridization of the input nucleic acid to the hairpin B and its opening, and the concomitant hybridization of (40) to hairpin C that resulted its opening. As before, these hybridization processes activated the catalytic structure of the “right” deoxyribozyme, while retaining the “left” part of the template in a catalytically inactive structure. Thus, the treatment of the  $i_2$ -activated structure of the reporter substrate (43) enabled the cleavage of the RNA nucleobase site, and the activation of the fluorescence from the TAMRA label. That is, the treatment of the template with the inputs (0, 1) resulted in a true output “1”. Finally, the treatment of the template (42) with the two inputs  $i_1$  and  $i_2$  resulted in the concomitant hybridization of the inputs with all four-hairpin regions of the template (42).

While input  $i_1$  hybridized with hairpins A and D and opened the two structures, the input  $i_2$  hybridized with hairpins B and C and opened these hairpin structures, respectively. The simultaneous hybridization processes stimulated by  $i_1$  and  $i_2$  distorted the template to a catalytically inactive configuration of the two deoxyribozyme units. As a result, the substrate (43) could not be cleaved and no fluorescence was generated. That is, the treatment of the template with the two inputs  $i_1$  and  $i_2$  (1, 1) resulted in a false output “0”. In terms of logic gate operations, the template performed the “XOR” gate functions. The combination of the AND and XOR gates allow the arithmetic half-adder operation. Fig. 9(c) shows the truth table for the half-adder. While the AND gate provides the carry digit C, the “XOR” output provides the sum digit. Other deoxyribozyme-based logic gates that perform Boolean functions and operate by related principles were constructed.<sup>54,55</sup> In these systems, nucleic acid sequences act as inputs for the partial or complete opening of pre-tailored hairpin-rich DNA templates. The catalytic functions of the ribozyme structures were regulated by the hybridization of the input-nucleic acids with the DNA templates, and the logic gate operations of the systems were readout by the fluorescence function of the cleaved substrate.

DNAzymes were also used to construct molecular motors that reveal open-close dynamic motion<sup>56,57</sup> or “walking” capabilities.<sup>58,59</sup> An autonomous DNA nanomotor that performed a continuous open–close dynamic motion with the aid of the  $\text{Mg}^{2+}$ -dependent “10–23” RNA cleaving DNAzyme was demonstrated<sup>56</sup> (Fig. 10(a)). The nucleic acid hybrid (44)/

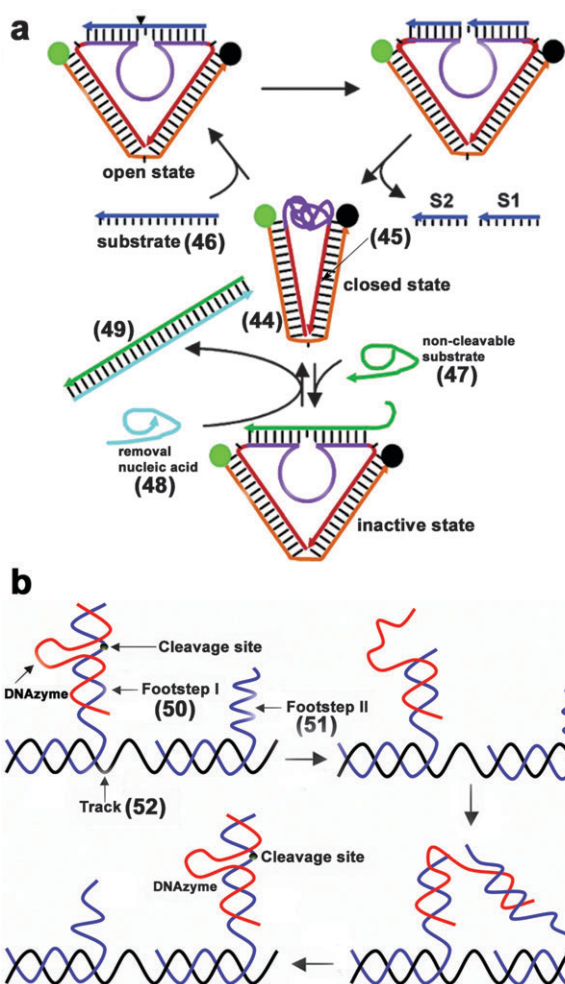


**Fig. 10** (a) A DNA-based nanomotor activated by the  $Mg^{2+}$ -dependent DNAzyme. (Reprinted with permission from ref. 56. Copyright 2004, American Chemical Society). (b) A “DNA walker” activated by the  $Mg^{2+}$ -dependent DNAzyme. (Reproduced with permission from ref. 59. Y. Tian *et al.*, A DNAzyme that walks processively and autonomously along a one-dimensional track, *Angew. Chem., Int. Ed.*, 2005, **44**, 4355. Copyright 2005, Wiley-VCH Verlag GmbH & Co.KGaA).

(45) was composed of a closed-state duplex that included a single-stranded flexible capping chain with the  $Mg^{2+}$ -dependent sequence-specific DNAzyme. Upon hybridization with the fuel substrate (46), the system adapted an extended “open” configuration, while the active cleaving enzyme configuration was formed. The scission of the substrate resulted in the spontaneous thermal separation of the cleaved nucleic acid units because of the low number of base-pairing, and the regeneration of the closed DNA motor device. Thus, as long as the “fuel” substrate was available in the system, its autonomous cleavage proceeded while moving the motor between “open” and “closed” structures, respectively. The “frame DNA” of the machine was substituted with a fluorophore-quencher pair that resulted in the fluorescence quenching of the dye in the “closed” state and the fluorescence enhancement in the “open” configuration. The introduction of a non-cleavable substrate (47) blocked the extended configuration,

and the motor functions of the molecular device were stopped.<sup>56</sup> In order to re-activate the machine, the non-cleavable substrate was removed by the complementary nucleic acid (48) that generated a duplex structure of increased stability.<sup>49</sup>

The “walking” of a DNAzyme along a DNA track was similarly demonstrated with the “10–23” DNAzyme,<sup>59</sup> and this is depicted in Fig. 10(b) with the migration of a DNA strand from one footstep to the other. Two DNA strands, the footsteps, (50) and (51), were linked to the nucleic acid track (52). The DNAzyme was hybridized with footstep I (50), and the enhanced stability of the resulting double strand favored this site of duplex formation. Cleavage of the footstep by the DNAzyme separated the cleaved nucleic acid, and the resulting single-strand migrated to footstep II, (51), while being hybridized. The duplex structure associated with footstep I underwent the subsequent de-hybridization and re-hybridization with footstep II due to the enhanced stability of the double-strand associated with footstep II. The subsequent scission of footstep II by the DNAzyme enabled the further “walking” of the DNAzyme on the “track”, and up to three migration steps were realized. The application of aptamers and DNAzymes for logic gate operations, and “motor” (walker) uses, is at this level of research only of basic interest. One might, however, envisage new scientific opportunities with these “smart” materials. For example, the combination of aptamers on pre-designed “walking tracks” could involve the activation of the “walking” process of anti-biomarker aptamers, and the concomitant release of tailored nucleic acids. Such “motoric walkers” may, then, release an anti-sense agents, and provide a new therapeutic paradigm.

## Conclusions and perspectives

Catalytic nucleic acids, DNAzymes, find growing interest in sensor applications, nanotechnology and logic gate operations. DNAzymes exhibit enhanced thermal stability as compared to enzymes. This property, together with the possibility to synthesize large quantities of DNAzymes, point to their potential for numerous applications. The use of DNAzymes as catalytic labels for amplified biosensing has already been established, and novel sensors that include DNAzyme-labeled hairpins or aptamer–DNAzyme conjugates have recently been developed. Particularly interesting are the molecular DNA machines that synthesize DNAzyme units as a result of sensing events. These systems revealed high sensitivities and represent isothermal, inexpensive and easy-to-operate assays, which could substitute the PCR process for many applications. The uses of such systems for rapid point-of-care diagnostics, or field tests of environmental pollutants or homeland security agents, such as pathogens, are envisaged. The use of aptamer-based DNA machines for amplified biosensing by the analyte-triggered synthesis of DNAzyme units is particularly interesting and represents major advantages over the PCR method that is limited for the amplification of nucleic acids only. The availability of aptamers for low-molecular-weight substrates, such as cocaine or antibiotics or for proteins such as thrombin or toxins allows, in principle, the activation of DNA machines that synthesize DNAzymes that provide a versatile tool to

analyze numerous substances. Indeed, this activation of a DNA machine by an aptamer–cocaine complex was recently reported.<sup>60</sup> Besides the use of DNazymes as catalytic labels for sensing, their application as functional tools in nanobiotechnology and for logic gate and computing is attractive. Although the examples for using DNazymes in these research areas are still scarce, systems of enhanced complexity that synthesize nanoscale devices, or perform coupled sensor and motor functions, or motor and computing functions, are anticipated to emerge.

The use of DNazymes as amplifying reporter units in biosensing is a ripe technology, and commercial assays using these biocatalysts are anticipated to appear on the market in the near future. Although the other applications of DNazymes are at the basic research level, the rapid progress in the field and the multidisciplinary applications of these biocatalytic materials hold great promises for additional developments.

## Acknowledgements

Our research on DNazymes and DNA machines is supported by the Johnson & Johnson Corporation.

## References

- 1 A. D. Ellington and J. W. Szostak, *Nature*, 1990, **346**, 818–822.
- 2 C. Tuerk and L. Gold, *Science*, 1990, **249**, 505–510.
- 3 I. Willner and M. Zayats, *Angew. Chem., Int. Ed.*, 2007, **46**, 6408–6418.
- 4 Y. Lu and J. Liu, *Curr. Opin. Biotechnol.*, 2006, **17**, 580–588.
- 5 Y. Lu and J. Liu, *Acc. Chem. Res.*, 2007, **40**, 315–323.
- 6 P. Travascio, P. K. Witting, A. G. Mauk and D. Sen, *J. Am. Chem. Soc.*, 2001, **123**, 1337–1348.
- 7 P. K. Witting, P. Travascio, D. Sen and A. G. Mauk, *Inorg. Chem.*, 2001, **40**, 5017–5023.
- 8 P. Travascio, Y. F. Li and D. Sen, *Chem. Biol.*, 1998, **5**, 505–517.
- 9 Y. Xiao, V. Pavlov, R. Gill, T. Bourenko and I. Willner, *ChemBioChem*, 2004, **5**, 374–379.
- 10 Y. Xiao, V. Pavlov, T. Niazov, A. Dishon, M. Kotler and I. Willner, *J. Am. Chem. Soc.*, 2004, **126**, 7430–7431.
- 11 E. H. Blackburn, *Cell*, 2001, **106**, 661–673.
- 12 J. Linger, T. R. Hughes, A. Shevchenko, M. Mann, V. Lundblad and T. R. Cech, *Science*, 1997, **276**, 561–567.
- 13 V. Pavlov, Y. Xiao, R. Gill, A. Dishon, M. Kotler and I. Willner, *Anal. Chem.*, 2004, **76**, 2152–2156.
- 14 T. Niazov, V. Pavlov, Y. Xiao, R. Gill and I. Willner, *Nano Lett.*, 2004, **4**, 1683–1687.
- 15 R. R. Breaker and G. F. Joyce, *Trends Biotechnol.*, 1994, **12**, 268–275.
- 16 J. Tang and R. R. Breaker, *Proc. Natl. Acad. Sci. U. S. A.*, 2000, **97**, 5784–5789.
- 17 J. W. Liu, A. K. Brown, X. L. Meng, D. M. Cropek, J. D. Istok, D. B. Watson and Y. Lu, *Proc. Natl. Acad. Sci. U. S. A.*, 2007, **104**, 2056–2061.
- 18 J. Liu and Y. Lu, *J. Am. Chem. Soc.*, 2007, **129**, 9838–9839.
- 19 A. Roth and R. R. Breaker, *Proc. Natl. Acad. Sci. U. S. A.*, 1998, **95**, 6027–6031.
- 20 S. Sando, T. Sasaki, K. Kanatani and Y. Aoyama, *J. Am. Chem. Soc.*, 2003, **125**, 15720–15721.
- 21 J. Liu and Y. Lu, *J. Am. Chem. Soc.*, 2003, **125**, 6642–6643.
- 22 C. B. Swearingen, D. P. Wernette, D. M. Cropek, Y. Lu, J. V. Sweedler and P. W. Bohn, *Anal. Chem.*, 2005, **77**, 442–448.
- 23 Y. Xiao, A. A. Rowe and K. W. Plaxco, *J. Am. Chem. Soc.*, 2007, **129**, 262–263.
- 24 K. A. Shaikh, K. S. Ryu, E. D. Goluch, J. M. Nam, J. W. Liu, S. Thaxton, T. N. Chiesl, A. E. Barron, Y. Lu, C. A. Mirkin and C. Liu, *Proc. Natl. Acad. Sci. U. S. A.*, 2005, **102**, 9745–9750.
- 25 J. Liu and Y. Lu, *Chem. Commun.*, 2007, 4872–4874.
- 26 M. N. Stojanović, P. de Prada and D. W. Landry, *J. Am. Chem. Soc.*, 2000, **122**, 11547–11549.
- 27 C. T. Lauhon and J. W. Szostak, *J. Am. Chem. Soc.*, 1995, **117**, 1246–1257.
- 28 P. Burgstaller and M. Famulok, *Angew. Chem., Int. Ed. Engl.*, 1994, **33**, 1084–1087.
- 29 D. E. Huizenga and J. W. Szostak, *Biochemistry*, 1995, **34**, 656–665.
- 30 J. F. Lee, G. M. Stovall and A. D. Ellington, *Curr. Opin. Chem. Biol.*, 2006, **10**, 282–289.
- 31 W. G. Purschke, F. Radtke, F. Kleinjung and S. Klussmann, *Nucleic Acids Res.*, 2003, **31**, 3027–3032.
- 32 J. Liu and Y. Lu, *Anal. Chem.*, 2004, **76**, 1627–1632.
- 33 D. Li, B. Shlyahovsky, J. Elbaz and I. Willner, *J. Am. Chem. Soc.*, 2007, **129**, 5804–5805.
- 34 C. X. Lin, Y. Liu, S. Rinker and H. Yan, *ChemPhysChem*, 2006, **7**, 1641–1647.
- 35 N. C. Seeman, *Trends Biochem. Sci.*, 2005, **30**, 119–125.
- 36 M. Beissenhirtz and I. Willner, *Org. Biomol. Chem.*, 2006, **4**, 3392–3401.
- 37 J. Bath and A. J. Turberfield, *Nat. Nanotechnol.*, 2007, **2**, 275–284.
- 38 Y. Tian and C. Mao, *J. Am. Chem. Soc.*, 2004, **126**, 11410–11411.
- 39 Y. Tian, Y. He and C. D. Mao, *ChemBioChem*, 2006, **7**, 1862–1864.
- 40 Z. Cheglakov, Y. Weizmann, B. Basnar and I. Willner, *Org. Biomol. Chem.*, 2007, **5**, 223–225.
- 41 Y. Weizmann, M. K. Beissenhirtz, Z. Cheglakov, R. Nowarski, M. Kotler and I. Willner, *Angew. Chem., Int. Ed.*, 2006, **45**, 7384–7388.
- 42 Z. Cheglakov, Y. Weizmann, M. K. Beissenhirtz and I. Willner, *Chem. Commun.*, 2006, 3205–3207.
- 43 A. Solinas, L. J. Brown, C. McKeen, J. M. Mellor, J. T. G. Nicol, N. Thelwell and T. Brown, *Nucleic Acids Res.*, 2001, **29**, E96.
- 44 N. L. Rosi and C. A. Mirkin, *Chem. Rev.*, 2005, **105**, 1547–1562.
- 45 J. W. Liu, D. P. Wernette and Y. Lu, *Angew. Chem., Int. Ed.*, 2005, **44**, 7290–7293.
- 46 A. P. De Silva and S. Uchiyama, *Nat. Nanotechnol.*, 2007, **2**, 399–410.
- 47 R. Baron, O. Lioubashevsky, E. Katz, T. Niazov and I. Willner, *Angew. Chem., Int. Ed.*, 2006, **45**, 1572–1576.
- 48 E. Shapiro and B. Gill, *Nat. Nanotechnol.*, 2007, **2**, 84–85.
- 49 Y. Chen, S. H. Lee and C. Mao, *Angew. Chem., Int. Ed.*, 2004, **43**, 3554–3557.
- 50 Y. Chen and C. Mao, *J. Am. Chem. Soc.*, 2004, **126**, 13240–13241.
- 51 G. Seelig, D. Soloveichik, D. Y. Zhang and E. Winfree, *Science*, 2006, **314**, 1585–1588.
- 52 W. Yoshida and Y. Yokobayashi, *Chem. Commun.*, 2007, 195–197.
- 53 M. N. Stojanović and D. Stefanović, *J. Am. Chem. Soc.*, 2003, **125**, 6673–6676.
- 54 M. N. Stojanović, T. E. Mitchell and D. Stefanović, *J. Am. Chem. Soc.*, 2002, **124**, 3555–3561.
- 55 H. Lederman, J. Macdonald, D. Stefanović and M. N. Stojanović, *Biochemistry*, 2006, **45**, 1194–1199.
- 56 Y. Chen and C. Mao, *J. Am. Chem. Soc.*, 2004, **126**, 8626–8627.
- 57 B. Yurke, A. J. Turberfield, A. P. Mills, F. C. Simmel and J. L. Neumann, *Nature*, 2000, **406**, 605–608.
- 58 J. Bath, S. J. Green and A. J. Turberfield, *Angew. Chem., Int. Ed.*, 2005, **44**, 4358–4361.
- 59 Y. Tian, Y. He, Y. Chen, P. Yin and C. D. Mao, *Angew. Chem., Int. Ed.*, 2005, **44**, 4355–4358.
- 60 B. Shlyahovsky, D. Li, Y. Weizmann, R. Nowarski, M. Kotler and I. Willner, *J. Am. Chem. Soc.*, 2007, **129**, 3814–3815.